https://doi.org/10.5194/nhess-2021-62
Preprint. Discussion started: 24 March 2021

Natural Hazards and Earth System Sciences
Discussions

Identifying plausible historical scenarios for coupled lake level and seismicity rate changes: The case for the Dead Sea during the last two millennia.

Mariana Belferman[1], Amotz Agnon[2], Regina Katsman[1] and Zvi Ben-Avraham[1]

[1] *The Dr. Moses Strauss Department of Marine Geosciences, Leon H. Charney School of Marine Sciences, University of Haifa, Mt. Carmel, Haifa 3498838, Israel.*

[2] *The Fredy & Nadine Herrmann Institute of Earth Sciences, The Hebrew University of Jerusalem, Jerusalem 9190401, Israel*

Mariana Belferman: mkukuliev@gmail.com (corresponding outhor)

Amotz Agnon: amotz@mail.huji.ac.il

Regina Katsman: rkatsman@univ.haifa.ac.il

Zvi Ben-Avraham: zviba@post.tau.ac.il

ABSTRACT

Seismicity triggered by water level changes in reservoirs and lakes is usually studied from well-documented contemporary records. Can such triggering be explored on a historical time scale when the data gathered on water level fluctuations in historic lakes and the earthquake catalogs suffer from severe uncertainties? These uncertainties stem from the different nature of the data gathered, methods, and their resolution. In this article, we considerably improve the correlation between the continuous record of historic water level reconstructions at the Dead Sea and discrete seismicity patterns in the area over the period of the past two millennia. Constricted by the data from previous studies, we generate an ensemble of random water level curves and

Natural Hazards and Earth System Sciences Discussions
Open Access

choose that curve that best correlates with the historical records of seismic stress release in the Dead Sea reflected in the destruction in Jerusalem. We then numerically simulate a synthetic earthquake catalog using this curve. The earthquakes of this synthetic catalog show an impressing agreement with historic earthquake records from the field. We demonstrate for the first time that water level changes correlate well with the observed recurrence interval record of historic earthquakes.

KEYWORDS

Seismic recurrence interval; Water level changes; Effective stress; Dead Sea

INTRODUCTION

Triggering of earthquakes by water level changes has been a focus of seismic investigations conducted all over the world (e.g. Simpson et al., 1988; Pandey and Chadha, 2003; Durá-Gómez and Talwani, 2010). It is attributed to the effective normal stress change at a fault, induced by the water load change at the overlying lake's bed (Simpson et al., 1988; Durá-Gómez and Talwani, 2010; Hua et al., 2013b; Gupta, 2018). This kind of triggering may be particularly significant for areas with moderate and low tectonic strain accumulations (Pandey and Chadha, 2003; Gupta, 2018), such as the Dead Sea fault in the Middle East (e.g. Masson et al., 2015).

Seismic activity due to water level change was observed beneath artificial reservoirs immediately after their first filling (e.g. Simpson et al., 1988; Hua et al., 2013 a). It also appeared after several seasonal filling cycles (Simpson et al., 1988; Talwani, 1997), explained by pore pressure diffusion to the earthquake's hypocentral depth via the fault (Durá-Gómez and Talwani, 2010). The correspondence of this kind of contemporary seismicity to water level change is usually identified based upon real-time data.

Alternatively, on a much longer time scale, changing seismic activity may also be associated with water level changes in historic water bodies (e.g the Dead Sea, 4 ka-present, Fig. 1A, which occupies the tectonic depression along the Dead Sea fault). Water level hikes of ~15 m, characteristic for time intervals of centuries to millennia, were analyzed in Belferman et al., (2018) and shown to be able to moderately represent the seismicity pattern at the Dead Sea fault (Belferman et al., 2018).

However, fluctuations in historic lake levels and the concurrent seismicity both include significant uncertainties. They stem from the differing nature of the data gathered on these two phenomena, and thus deserve special consideration. Earthquake dating can be quite precise, and its accuracy can be verified when different historical sources show consensus (Guidoboni et al., 1994; Guidoboni and Comastri, 2005; Ambraseys, 2009). Assessment of the extent of damage (hence earthquake magnitude), similarly requires such a consensus between the different data sources. Sediment records can help to calibrate the analysis of the historical evidence (Agnon, 2014; Kagan et al., 2011). Such records can be tested by trenching (Klinger et al., 2015; Lefevre, 2018). However, in many cases location of the earthquake epicenter can be imprecise or not even known.

By contrast, historic water level records are quite precise, as they are obtained from different points around the lake (Bookman et al., 2004; Migowski et al., 2006). However, water level dating could have an error of about ±45 yr, as estimated from the radiocarbon dating of shoreline deposits in a fan delta outcrop (Bookman et al., 2004). This may underestimate the actual dating uncertainty

https://doi.org/10.5194/nhess-2021-62
Preprint. Discussion started: 24 March 2021

due to reworking of organic matter, sometimes re-deposited a century or more after equilibration with the atmosphere (Migowski et al., 2004). In addition, the entire past bi-millennial Dead Sea level record is constrained by less than twenty "anchor points" (the data obtained by the dating collected from surveyed paleo-shorelines, Bookman et al., 2004). Therefore, its continuous reconstruction, as suggested in the literature (Migowski et al., 2006; Stern, 2010), usually takes different forms within the acceptable limits dictated by the limnological evidence (Bookman et al., 2004). A challenging uncertainty for our study arises from periods when the available data does not constrain the water levels.

In this article, we take advantage of the correlation between the historic water level reconstructions at the Dead Sea and seismicity patterns in the area over the past two millennia. We demonstrate for the first time that plausible scenarios for the lake level history can fit very well the record of the historic earthquakes RI. The fit can even be improved when moderate local earthquakes are considered for stress release history.

METHODS

To investigate the relation between an accurate but discrete chronology of earthquakes and the continuous water level (WL) change, we first explore the space of possible WL histories by a statistical approach. We generate an ensemble of WL curves based on the anchor points (Bookman et al., 2004), while remaining within the limits dictated by climatic and morphological constraints (Bookman et al., 2004; Migowski et al., 2006 and Stern, 2010), by using a random number generator.

Best fit random method of WL curve prediction

https://doi.org/10.5194/nhess-2021-62
Preprint. Discussion started: 24 March 2021

The compilation of WL curves of the Dead Sea for the last two millennia from three recent publications (Bookman et al., 2004; Migowski et al., 2006 and Stern 2010) is presented in Figure 1A by dashed lines. Generally, the differences between all dashed curves at anchor points is included within an error limit of ±45 yr as indicated by error bars, with the exception of the anchor point dated to 1400 CE (Bookman et al., 2004) for which Migowski et al. (2006) and Stern (2010) suggested a higher WL. Nevertheless, each hypothetical WL curve is forced to pass through all anchor points according to Bookman et al. (2004) except for one, at around 500 CE. The WL drop around this time, according to Migowski et al. (2006) and Stern (2010), occurred later than was originally suggested by Bookman et al. (2004) (Figure 1A). Because this shift is within the permissible error limits (±45 yr), this anchor point is shifted to the left (+40 yr). In addition, the WL determined on the edges of the studied bi-millennial time interval was fixed by an additional 2 points, through which the estimated WL curve passed according to all three references specified above. In total, we have 13 anchor points. Between each pair of points, the trend in the WLs is constrained by the sedimentary facies (Migowski et al., 2006) that specify the edge points of the interval as the extrema for the acceptable WL variation.

However, within the largest interval between the anchor points (600 - 1100 CE), the on-land studies (Migowski et al., 2006; Stern, 2010; Bookman et al., 2004) constrained the WL to be lower than the extrema at the edges of that interval. For this period, the WL was randomly interpolated between the suggested maximum (Migowski et al., 2006) and minimum (e.g. Stern, 2010). To maintain a monotony of the WL variation, a moving average filtered the random noise between every pair of anchor points. Accounting for the above-mentioned limits, and setting a ten-year step, the model generates 10 Million WL curves for the last bi-millenial interval, using a uniformly distributed random number generator.

https://doi.org/10.5194/nhess-2021-62
Preprint. Discussion started: 24 March 2021

The linear correlation between the recurrence intervals (RIs) of the widely recorded moderate-to-large (M>5.5) historical earthquakes available from the literature (see Table 1 and the text description in Appendix), and the generated WLs, was tested (e.g. as in Figure 9 in Belferman et al., 2018) by calculating the value of the Pearson product-moment correlation coefficient, R (Figure 2B). We use these statistics for evaluating the suitability of each randomly interpolated WL curve for our analysis, for identification and elimination of any outliers, and for studying the behavior of the entire ensemble of the curves generated.

The earthquake simulation algorithm

The most suitable WL curve suggested by this correlation (discussed in the results section below), was used to generate a "Synthetic" earthquakes catalog based on the algorithm described in this section. Synthetic earthquakes are simulated in the model by superimposing the effective normal stress change due to the WL change on the tectonic stress accumulated since the preceding seismic event. An array of WL change, $\Delta h_i (i = 1,2, \dots 2000)$, was generated. Using this array, another array of effective normal stress changes, $\Delta\sigma_i'$, at the fault, induced by water load change at the lake's bed, p_{s_i}, is calculated as:

1. $$\Delta\sigma_i' = \frac{1-2\nu}{1-\nu}(\beta - 1)p_{s_i}$$

(Eq. 10b in Belferman et all., 2018). This equation assumes the post-diffusion stage: i.e. when pore pressure at the hypocentral depth approaches the value at the lake's bed. Here β is Biot's coefficient and ν is the Poisson's ratio, $p_{s_i} = \rho g \Delta h_i$, where ρ is the density of water and g is the acceleration of gravity.

The model uses a Byerlee's law envelope (Byerlee, 1978) to define the strength of a seismogenic zone at the fault immediately after the earthquake (see Belferman et al., 2018 for more

https://doi.org/10.5194/nhess-2021-62
Preprint. Discussion started: 24 March 2021

Natural Hazards and Earth System Sciences
Open Access
Discussions

detail). The starting point of the simulations is the date of the first historic earthquake (33CE, see Table 1 in the Appendix) from the studied bi-millennial time interval. The simulation incrementally proceeds with time over the chosen WL curve (as above) also considering the tectonic stress accumulation. After each stress release, the time to the next earthquake is calculated using the solution of the Mohr-Coulomb failure criterion for a strike-slip tectonic regime applicable to the Dead Sea fault (Belferman, et al., 2018):

$$(\tau_i - \tau_0)^2 + \left(\sigma_i - (\sigma_0 + \Delta\sigma_i')\right)^2 = \left(R_0 + \Delta\tau_{xy_i}\right)^2 \tag{2}$$

$$\tau_i = C + tan(\varphi)\sigma_i$$

assuming that $\Delta\tau_{xy_i} = \frac{Ccos(\varphi)}{t_{RI}}\Delta t$ is the tectonic shear stress at the strike-slip fault accumulated during the period Δt (time passed since the last earthquake), C is cohesion, φ is an angle of internal friction, σ_0 and τ_0 are the coordinates of the Mohr circle immediately after the earthquake and R_0 its radius, t_{RI} is the reference RI corresponding to the minimal WL.

For each time step, the algorithm determines whether there is a single solution, or two, or no solutions. A case of no solutions means that the Mohr circle is yet to reach the failure envelope, as the accumulated tectonic stress and the WL increase are still insufficient. The system of Eq. 2 may have one solution when an earthquake occurs at the end of some step in time or two solutions when the failure criterion is met before the end of the time step. A case of two solutions is rounded down to a case of a single solution ifa time step (one year) is small compared to the earthquake RI (several hundreds of years).

This solution of Eq.2 yields a RI as a function of the effective normal stress change, $\Delta\sigma_i'$ (Belferman et al., 2018):

https://doi.org/10.5194/nhess-2021-62
Preprint. Discussion started: 24 March 2021

3. $$RI = \Delta t = (C + tan(\varphi)\Delta\sigma_i')\frac{t_{RI}}{C}$$

where t_{RI} is the reference RI corresponding to the minimal WL, C is cohesion, φ is an angle of internal friction. From this formula for RI, the array of earthquake dates is obtained.

Substituting Eq.1 into Eq.3, we get a simulated RI as a linear function of WL change with time, Δh_i.

4. $$RI = t_{RI} + \frac{tan(\varphi)}{C}\frac{1-2\nu}{1-\nu}(\beta - 1)\rho g t_{RI}\Delta h_i$$

Coefficients for the simulations were previously determined in Belferman et al. (2018). In addition, a left-lateral strike-slip tectonic motion at the Dead Sea fault with a constant velocity of ~5 mm/yr (e.g. Masson et al., 2015) is used. The change in WL is calculated relative to its minimal level (415 m bmsl) over the period. A cohesion value, $C = 0.08 Mpa$ and a reference RI, $t_{RI} = 300 yr$, were adjusted numerically for specific WL curve, providing the average RI of 144 yr over the modelled period of two millennia justified by historical data (Agnon, 2014).

RESULTS

The best fit WL curve (black solid line in Figure 1A) was identified out of the 10M random set of WL curves by the Pearson product-moment correlation test. The values of correlation coefficients, R, for the entire ensemble of randomly interpolated WLs are distributed normally around R=0.63 (Figure 1B) with a standard deviation of σ =0.076.

Three outliers from the thirteen RIs of the widely recorded historic earthquakes (749 CE, 1293 CE, 1834 CE) were identified and reevaluated (Figure 1D). A curve with a highest Pearson coefficient of R=0.912 was chosen from the correlation between the RIs of the revised historic

https://doi.org/10.5194/nhess-2021-62
Preprint. Discussion started: 24 March 2021

Natural Hazards and Earth System Sciences Discussions
Open Access EGU

catalog and the randomly generated WLs. This correlation can be specified by a linear prediction function

5. $$RI = -5442 - 14WL$$

where RI is given in years and WL in meters. In addition, a synthetic earthquake history including 14 seismic events was simulated from the chosen randomly interpolated WL curve with R=1 specified above. The correlation between the synthetic RIs and WLs (presented in Figure 1C) is:

6. $$RI = -3840 - 10WL$$

as expected from the linear dependence suggested by the analytical solution (Eq.4). The dates of the simulated synthetic earthquakes are presented, versus the dates of the historic earthquakes from the literature (Table A1, Appendix) in Figure 1E.

https://doi.org/10.5194/nhess-2021-62
Preprint. Discussion started: 24 March 2021

Natural Hazards and Earth System Sciences
Discussions

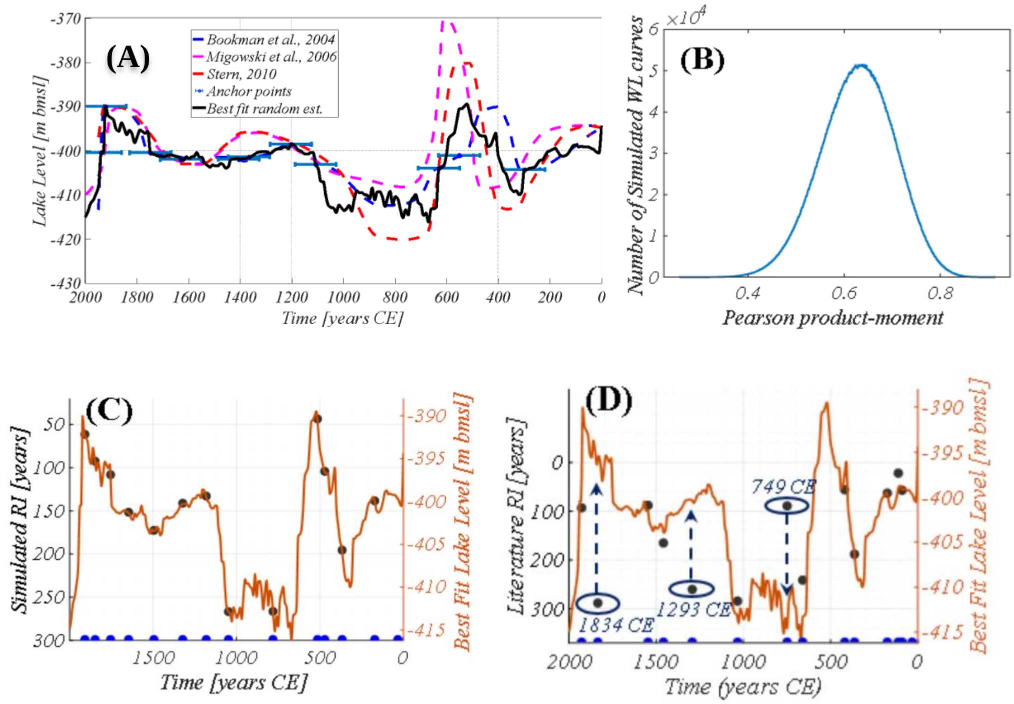

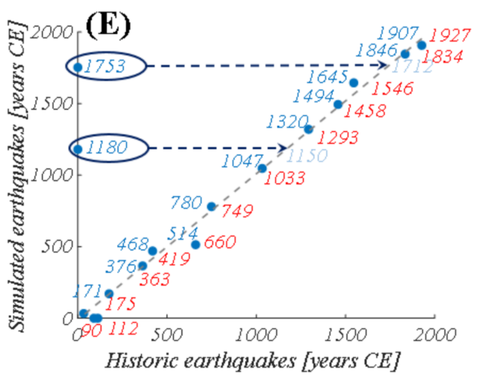

Figure 1: ***(A)*** *The Dead Sea WL reconstruction for the last two millennia. The dashed curves are suggested by the literature sources. Blue anchor points with an error interval of ±45 yr. follow Bookman et al. (2004). Solid, black line water curve is suggested by this study.* ***(B)*** *Distribution of Pearson's product-moment correlation coefficient of randomly interpolated WLs and RIs of historic earthquakes. Normal distribution results from 10M random WLs reconstructions.* ***(C)*** *and* ***(D):*** *Chosen best fit random WL curve vs. simulated and historic RIs, correspondingly.* ***(E)*** *Dates of historic vs. simulated earthquakes based on the suggested best fit WLs curve (Figs.C,D).*

https://doi.org/10.5194/nhess-2021-62
Preprint. Discussion started: 24 March 2021

Natural Hazards and Earth System Sciences
Discussions

DISCUSSION

Uncertainties in the WL reconstructions associated with dating and resolution lead to considerable variance in possible interpolations (Figure 1B). A Pearson correlation coefficient test shows that most of the randomly interpolated WL curves give linear correlation with earthquake RIs (indicated by a mean Pearson coefficient of R=0.63), excluding the three outliers (Figure 1D) to be discussed below.

For simulating synthetic earthquakes triggered by WL change, we use the WL curve that generates the highest correlation with the revised historical catalog (R = 0.912). The dates of these simulated synthetic earthquakes are comparable with historical earthquakes (Figure 1E) excluding two events, whose dates are shifted to the y-axis for clarity of presentation (1753 CE, 1180 CE). The dates of these synthetic earthquakes might be connected to three outliers from the historical catalog (1834 CE, 1293 CE, 749 CE depicted in Figure 1D) as explained below.

The 1180 CE synthetic earthquake (Figure 1E) is comparable to an earthquake in the - literature dated by Ben-Menachem (1979) and Amiran et al. (1994) to the mid-12th century (~1150 CE). Ambraseys (2009) doubted the precise dating but accepted this mid-12th century estimate. The damaged area of this earthquake spanned Jericho and Jerusalem, and the event could be considered as significant, because it led to the total destruction of two monasteries, one of which is 10 km south of Jerusalem's curtain wall. By admitting the ~1150 CE earthquake to the amended catalog, we reduce the RI of the subsequent earthquake at 1293 CE (Figure 1D) from 260 to 143 yrs, thereby bringing this outlier very close to the linear correlation.

Our model also generates an earthquake in the 18th century, dated 1753 CE, for which there were no matches in our initial historical catalog. However, in Amiran's et al. (1994) catalog an

https://doi.org/10.5194/nhess-2021-62
Preprint. Discussion started: 24 March 2021

earthquake in 1712 CE is indicated: 'The quake shook the solid houses and ruined three Turkish houses. Felt in Ramle, but not in Jaffa'. Additionally, this earthquake is evidenced by seismites dated to 1700 – 1712 CE from an Ein Gedi site (Migowski et al., 2004).

Regarding the modeled 1907 CE event, we note the well documented (although often overlooked) 29 March 1903 CE earthquake (Amiran et al., 1994). This was a moderate but extended earthquake: local intensity reached VII in a number of localities distributed outside the rift valley over an area of 140x70 square km (including Jerusalem), whereas the maximum intensity reported in the rift was VII as well (Jericho). We prefer to correlate the modeled 1907 event with the stronger 1927 Jericho earthquake that clearly released stress in the Dead Sea (e.g. Shapira, et al., 1993; Avni et al., 2002; Agnon, 2014). This leaves the 1903 unmatched to our model. Perhaps the earthquake ruptured the northern part of the central Jordan Valley, north of the Dead Sea and south of Lake Kinneret (Sea of Galilee).

Regarding the last outlier from the historical earthquakes dated to 749 CE (or its neighbors 747 and 757, Table A1 in the Appendix) (Figure 1D) and corresponding to the simulated 780 CE earthquake (Figure 1E): the simulation generated the preceding earthquake 514 CE associated with the 659/660 CE event from the literature (Table A1 in the Appendix) with a deviation of 146 years. The rupture zone of 659/660 CE event is uncertain, and this earthquake is not necessarily related to stress release at the Dead Sea basin. Alternatively, following Russel (1985), as a result of the 551 CE earthquake, a fortresses east of the southern Dead Sea and Petra were destroyed. Newer data (Marco et al., 1996) contradicts the assertion regarding Petra; a failure at the Dead Sea region is still plausible. Replacing the 660 CE earthquake with 551 CE in the list of relevant historical earthquakes changes the RI preceding the 749 CE historical earthquake from 89 to 198, which brings this outlier into a satisfactory linear correlation (Figure 1D).

https://doi.org/10.5194/nhess-2021-62
Preprint. Discussion started: 24 March 2021

Natural Hazards and Earth System Sciences
Discussions

Additionally, it should be emphasized that in the simulation presented in this article, the starting point is, quite arbitrarily, the earthquake of 33CE. This event and the subsequent earthquakes 90CE and 112CE (not predicted by our model) span a single century. Each of these events could thus represent the starting point of the simulations, or could be omitted at this early and poorly documented interval.

Summarizing the above amendments, we add to our list of historic events the 551 CE, ~1150 CE, 1712 CE, earthquakes and remove 559/660 CE and 90CE, 112 CE earthquakes (Figure 1E). Altogether, we get 14 triggered historic earthquakes.

The RI of the resulting list of historical earthquakes linearly correlates with WL change. This is noticeable despite the different form of the water level curves (Figure 2).

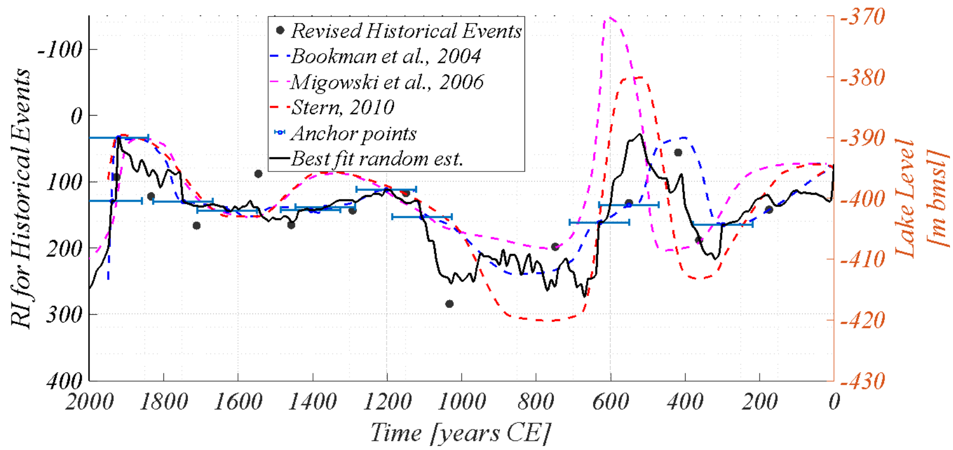

Figure 2: *The Dead Sea WL reconstruction for the last two millennia. The dashed curves are suggested by the literature. Blue anchor points with an error interval of ±45 yr follow Bookman et al. (2004). The solid black line is the water curve suggested by this study. The black points represent the RI for revised historical events, suggested in this study as being relevant to the Dead Sea area.*

https://doi.org/10.5194/nhess-2021-62
Preprint. Discussion started: 24 March 2021

The correlation of RI with best fit random estimated curve can be specified by a linear prediction function:

$$7. \qquad RI = -2483 - 6.5WL$$

Since the last earthquake (1927CE), the water level in the Dead Sea has continuously decreased at an average annual rate of ~1 m/yr. Today the water level is about -440 (m bmsl), thus our prediction function suggest an RI of 377 yr, for such a WL. More specifically, if the water level in the Dead Sea remained constant (-440 m bmsl), we would expect the next earthquake at about ~2300 yr. However, as the water level keeps falling, a moderate- to large-earthquake is predicted even later.

This paper stresses that reconstructions of WL curves are not unique and may take various forms under the constraints available (e.g. Figure 1A,). However, the correlation with an independent record of RIs of seismic events, assuming that earthquakes are affected by WL hikes, allows deciphering plausible scenarios for WL evolution. Moreover, for cases with the best but not perfect correlation, the deviation might be consistent with a release of elastic energy by smaller earthquakes, which are not accounted for by the deterministic part of our model. We note that smaller earthquakes might rupture dipping fault planes, again not accounted for by our simple model.

Our results demonstrate that a fairly simple forward model (based on 1D analytical solution, Belferman et al., 2018) achieves a very good correlation between WLs and RIs of moderate-to-strong earthquakes on the Dead Sea fault. Whereas the fault system along the Dead Sea fault is more complicated, three-dimensional modeling of the tectonic motion, coupled to the pore pressure evolution, may give more reliable predictions regarding the earthquake ruptures and their

https://doi.org/10.5194/nhess-2021-62
Preprint. Discussion started: 24 March 2021

chronology. Finally, we note that under the present man-induced decline of the Dead Sea level (at an average annual rate of ~1 m/y) a moderate- to large-earthquake will not be triggered by the mechanism discussed here.

ACKNOWLEDGMENTS

This project was supported by the grants from Ministry of Natural Infrastructures, Energy and Water Resources of Israel # *213-17-002*, and GIF- German - Israeli Foundation for Scientific Research and Development # I-1280-301.8. The data for this paper was obtained with analytical and numerical modeling.

REFERENCE

Agnon A. 2014. Pre-instrumental earthquakes along the Dead Sea rift. In Dead Sea transform fault system: reviews, edited by Garfunkel, Zvi, Ben-Avraham, Zvi, Kagan, Elisa, 207-261, Springer, Dordrecht. ***https://doi.org/10.1007/978-94-017-8872-4_8***.

Ambraseys, N. 2009. Earthquakes in the Mediterranean and Middle East: a multidisciplinary study of seismicity up to 1900. Cambridge University Press. doi: ***https://doi.org/10.1017/CBO9781139195430***

Ambraseys, N. N., Melville, C. P. and Adams, R. D. 1994. *The Seismicity of Egypt, Arabia and the Red Se: A Historical Review*. Cambridge: Cambridge Univ. Press. ***https://doi.org/10.1017/S1356186300007240***

Amiran, D. H., Arieh, E., and Turcotte, T. 1994. Earthquakes in Israel and adjacent areas: macroscopic observations since 100 B.C.E. *Israel Exploration Journal*, *44*, 260– 305. ***http://www.jstor.org/stable/27926357.***

https://doi.org/10.5194/nhess-2021-62
Preprint. Discussion started: 24 March 2021

Natural Hazards and Earth System Sciences
Open Access
Discussions

Avni, R., Bowman, D., Shapira, A. and Nur, A. 2002. Erroneous interpretation of historical documents related to the epicenter of the 1927 Jericho earthquake in the Holy Land. *Journal of seismology*, 6(4), 469-476. ***https://doi.org/10.1023/A:1021191824396***

Belferman, M., Katsman, R. and Agnon, A. 2018. Effect of large-scale surface water level fluctuations on earthquake recurrence interval under strike-slip faulting. *Tectonophysics*, 744, 390-402. ***https://doi.org/10.1016/j.tecto.2018.06.004***

Ben-Menahem, A. 1979. Earthquake catalogue for the Middle East (92 BC-1980 AD). *Boll. Geofis. Teor. Appl.*, 21, 245-313.

Bookman, R., Enzel, Y., Agnon, A., and Stein, M. 2004. Late Holocene lake levels of the Dead Sea. *Geological Society of America Bulletin* 116, 555-571. ***https://doi.org/10.1130/B25286.1***

Byerlee, J.D., 1978. Friction of rocks. In: Byerlee, J.D., Wyss, M. (Eds.), Rock Friction and Earthquake Prediction. *Springer, Birkhäuser, Basel*, pp. 615–626. ***https://doi.org/10.1007/978-3-0348-7182-2***

Durá-Gómez, I. and Talwani, P. 2010. Reservoir-induced seismicity associated with the Itoiz Reservoir, Spain: a case study, *Geophysical Journal International*, 181, 343–356. ***https://doi.org/10.1111/j.1365-246X.2009.04462.x***

Elad, A. 1982. An early arabic source concerning the markets of Jerusalem. *Cathedra*, 24, 31-40.

Elad, A., 1992. Two Identical Inscriptions From Jund Filastin From the Reign of the Abbāsid Caliph, Al-Muqtadir. *Journal of the Economic and Social History of the Orient*, *35*(4), 301-360. ***https://doi.org/10.2307/3632739***

https://doi.org/10.5194/nhess-2021-62
Preprint. Discussion started: 24 March 2021

Gerber, H., 1998. " Palestine" and Other Territorial Concepts in the 17th Century. *International Journal of Middle East Studies,* 30(4), 563-572. ***https://www.jstor.org/stable/164341***

Guidoboni, E., Comastri, A., and Traina, G. 1994. Catalogue of Ancient Earthquakes in the Mediterranean Area Up to the 10th Century. Rome: Istituto nazionale di geofisica. ***https://doi.org/10.1163/182539185X01377***

Guidoboni, E. and Comastri, A. 2005. Catalogue of Earthquakes and Tsunamis in the Mediterranean Area from the 11th to the 15th Century. Istituto nazionale di geofisica e vulcanologia. ***https://doi.org/10.1515/BYZS.2008.854***

Gupta, H., K., 2018, Reservoir triggered seismicity (RTS) at Koyna, India, over the past 50 yrs. *Bulletin of the Seismological Society of America* 108.5B: 2907-2918. ***https://doi.org/10.1785/0120180019***

Hua, W., Chen, Z. and Zheng, S., 2013a. Source parameters and scaling relations for reservoir induced seismicity in the Longtan reservoir area. Pure Appl. Geophys. 170, 767–783. ***https://doi.org/10.1007/s00024-012-0459-7***

Hua, W., Chen, Z., Zheng, S., and Yan, C., 2013b. Reservoir-induced seismicity in the Longtan reservoir, southwestern China. J. Seismol. 17 (2), 667–681. ***https://doi.org/10.1007/s10950-012-9345-0***

Hough S. E. and Avni R., 2011. The 1170 and 1202 CE Dead Sea Rift earthquakes and long-term magnitude distribution of the Dead Sea Fault Zone, *Isr. J. Earth Sci.*, 58, 295–308. ***ttps://doi.org/10.1560/IJES.58.3-4.295***

Kagan, E., Stein, M., Agnon, A., and Neumann, F. 2011. Intrabasin paleoearthquake and quiescence correlation of the late Holocene Dead Sea. Journal of Geophysical Research*:* *Solid Earth*, 116(B4). ***https://doi.org/10.1029/2010JB007452***

Ken-Tor, R., Agnon, A., Enzel, Y., Stein, M., Marco, S., and Negendank, J. F. 2001. High-resolution geological record of historic earthquakes in the Dead Sea basin. *Journal of Geophysical Research-Solid Earth, 106,* 2221-2234. ***https://doi.org/10.1029/2000JB900313***

Klinger, Y., Le Béon, M. and Al-Qaryouti, M., 2015. 5000 yr of paleoseismicity along the southern Dead Sea fault. Geophys. J. Int. 202 (1), 313–327. ***https://doi.org/10.1093/gji/ggv134***

Langgut, D., Yannai, E., Taxel, I., Agnon, A. and Marco, S., 2015. Resolving a historical earthquake date at Tel Yavneh (central Israel) using pollen seasonality. *Palynology*, *40(2)*, 145-159. ***https://doi.org/10.1080/01916122.2015.1035405***

Lefevre, M., Klinger, Y., Al-Qaryouti, M., Le Béon, M. and Moumani, K., 2018. Slip deficit and temporal clustering along the Dead Sea fault from paleoseismological investigations. Sci. Rep. 8 (1), 4511. ***https://doi.org/10.1038/s41598-018-22627-9***

Marco, S., Stein, M., Agnon, A., and Ron, H. 1996. Long-term earthquake clustering: A 50,000-year paleoseismic record in the Dead Sea Graben. Journal of Geophysical Research: Solid Earth, 101(B3), 6179-6191. ***https://doi.org/10.1029/95JB01587***

Masson, F., Hamiel, Y., Agnon, A., Klinger, Y. and Deprez, A., 2015. Variable behavior of the Dead Sea Fault along the southern Arava segment from GPS measurements. comptes rendus geoscience, 347(4), pp.161-169. ***https://doi.org/10.1016/j.crte.2014.11.001***

Migowski, C., Agnon, A., Bookman, R., Negendank, J. F., and Stein, M. 2004. Recurrence pattern of Holocene earthquakes along the Dead Sea transform revealed by varve-counting and radiocarbon dating of lacustrine sediments. *Earth and Planetary Science Letters, 222,* 301–314. ***https://doi.org/10.1016/j.epsl.2004.02.015***

Migowski, C., Stein, M., Prasad, S., Negendank, J. F. W., and Agnon, A. 2006. Holocene climate variability and cultural evolution in the Near East from the Dead Sea sedimentary record. *Quaternary Research*, 66(3), 421-431. ***https://doi.org/10.1016/j.yqres.2006.06.010***

Parker, S.T., 1982. Preliminary Report on the 1980 Season of the Central" Limes Arabicus" Project. *Bulletin of the American Schools of Oriental Research*, *247*(1), pp.1-26. ***https://www.journals.uchicago.edu/doi/10.2307/1356476***

Pandey, A.P. and Chadha, R.K., 2003. Surface loading and triggered earthquakes in the Koyna– Warna region, western India. *Phys. Earth Planet. Inter.* 139 (3 – 4), 207 – 223. ***http://dx.doi.org/10.1016/j.pepi.2003.08.003***

Russell, K. W., 1985. The earthquake chronology of Palestine and northwest Arabia from the 2nd through the mid-8th century AD. Bulletin of the American Schools of Oriental Research, 260(1), 37-59. ***https://doi.org/10.2307/1356863***

Shapira, A., Avni, R., and Nur, A. 1993. A new estimate for the epicenter of the Jericho earthquake of 11 July 1927. *Isr. J. Earth Sci,* 42(2), 93-96.

Simpson, D. W., Leith, W., and Scholz, C. 1988. Two types of reservoir-induced seismicity. *Bulletin of the Seismological Society of America, 78*, 2025–2040.

https://doi.org/10.5194/nhess-2021-62
Preprint. Discussion started: 24 March 2021

Stern, O. 2010. Geochemistry, Hydrology and Paleo-Hydrology of Ein Qedem Spring System; Report GSI/17/2010; Geological Survey of Israel: Jerusalem, Israel, 2010; p. 91. (In Hebrew)

Talwani, P., 1997. On the nature of reservoir-induced seismicity. Pure Appl. Geophys. 150, 473–492. ***https://doi.org/10.1007/978-3-0348-8814-1_8***

Williams, J. B., Schwab, M. J., & Brauer, A. 2012. An early first-century earthquake in the Dead Sea. *International Geology Review*, *54*(10), 1219-1228. ***https://doi.org/10.1080/00206814.2011.639996***

Appendix: The earthquake history of the Dead Sea environs

Numerous publications list earthquakes that hit the Dead Sea and its surroundings during the last two millennia (e.g. Agnon, 2014; Ambraseys et al., 1994; Ambraseys, 2009; Amiran et al., 1994; Guidoboni et al., 1994, Guidoboni and Comastri, 2005). In Belferman et al. (2018) we adopted from the scores of listed events only the most destructive ones, typically causing local intensities of VII or higher in Jerusalem. For a minimal epicentral distance of 30 km, this would translate to a magnitude of ~5.7 or higher (according to the attenuation relation of Hough and Avni, 2011).

Table A1 lists the Dead Sea earthquakes considered for stress release across the Dead Sea basin during the last two millennia. We used two criteria: noticeable damage in fortified Jerusalem, and seismites in the northern Dead Sea. Our simple model simulates an earthquake time series, given a water level curve. Eleven events from this time series correlate with events of magnitude ~6 or more in the historic record. Yet, the model generates four events that are not included in our original list. On the other hand, a single event (~660 CE) listed in Belferman et al. (2018) has no counterpart in the simulations despite a wide range of level curves tested. All these curves are

https://doi.org/10.5194/nhess-2021-62
Preprint. Discussion started: 24 March 2021

Natural Hazards and Earth System Sciences
Discussions

generated by a random number generator, subject to constraints from field data. We first discuss the four events required by the simulations one by one. Then we review the ~660 CE event along with other historic events that were left out already in Belferman et al. (2018).

The earthquakes in Table 1 are classified according to the level of acceptance for being destructive in Jerusalem. The nine events of **Class C** are all consensual, also used by Belferman et al.(2018). These events appear in all catalogues and lists, and need no further discussion. The six events of **Class A** are debated events, accepted in the present study. All earthquakes in this class are selected by simultaneously satisfying two criteria: (1) The acceptance regularizes the relation between recurrence intervals and lake level; (2) They are corroborated by evidence from seismites in the northern basin of the Dead Sea (Ein Feshkha and Ein Gedi sites, Fig.A1corroborate).

We chose the year **33** CE to start our simulations. While this earthquake did not cause a widespread damage, it was recorded in all three seismite sites (Kagan et al., 2011), with a maximum of decade uncertainty based on dating by counting lamina under the microscope (Migowski et al., 2004; Williams et al., 2012).

The second entry in Table A1, **~100** CE, refers to two decades of unrest. Migowski et al. (2004) identified a pair of seismites around 90 CE and 112 CE in the ‘Ein Gedi Core. The corresponding sequences in Ein Feshkha and Ze’elim Creek are laminates, attesting to quiescence. A historical hiatus between the Roman demolition of Jerusalem and the erection of Ilya Capitolina in its stead (70-130 CE) preclude historical evidence. Although damage to the Masada fortress has been assigned to an earthquake **1712 CE.**

Table A2 lists ten earthquakes that have been reported to damage around Jerusalem but are not required by our simulations. The seven events of **Class R** are the debated events, rejected here after discussion. The three **Class S** events were skipped altogether in that compilation of Ambraseys (2009).

Of the seven Class R events, the 7 June **659** CE earthquake was accepted by us in Belferman et al. (2018). The earthquake has been associated with destruction of the Euthymius monastry 10 km east of Jerusalem, but no damage in the town of Jerusalem has been unequivocally reported (Ambraseys, 2009). In Belferman et al. (2018) we included this event in the list of Dead Sea earthquakes, as Langgut et al. (2015) have located it on the center of the Jordan Valley segment of the transform (Figure A1). However, this interpretation neglected the possibility that the rupture could have been outside the hydrological effect of the Dead Sea basin. One of the lessons of our numerous simulations is that our model would not support triggering of this earthquake shortly (less than a century) before the mid-8th century crisis, when lake levels were dropping to the lowest point in the studied period (420 m bsl, Fig. 1a). When rejecting the 659 CE event, the 419 CE earthquake is the one preceding the mid-8th century crisis; the three century recurrence interval fits well the low lake level.

1016 CE: The collapse of the Dome of the Rock was not explicitly attributed to an earthquake by the original sources, who found it enigmatic as well (Ambraseys, 2009).

1644 CE: Ambraseys (2009) quoted a late Arab author, al-Umari, who reported collapse of houses and deaths of five persons in “the town of Filistin”. While Ambraseys has interpreted it probably to Jerusalem, it might refer to al-Ramla, the historical capital of the classical Filistin District, as in “al-Ramla, Madinat Filastin” (Elad, 1992, p335). Or, it is a mistranslation of “Bilad Filistin” which at that time started refer to the entire Holy Land district, without specifying a town (Gerber, 1998). Jerusalem, at that time, was called Bayt el Maqdis or, as nowadays, al-Quds. The only report of an earthquake in Jerusalem around 1644 mentions horror but no structural damage - the 1643 CE

https://doi.org/10.5194/nhess-2021-62
Preprint. Discussion started: 24 March 2021

event that Ambraseys (2009) tends to equate with the 1644 CE event. A seismite in Ein Gedi core can be correlated with this event (Migowski et al., 2004, Table 2, entry 6). Migowski et al. (2004) have identified the seismite with the 1656 earthquake that was felt in Palestine; Ambraseys' (2009) interpretation was not yet available for them.

1656 CE: This event was strong in Tripoli and only felt in Palestine. Migowski et al. (2004) correlated it to a seismite based on deposition rates (no lamina counting for that interval). Given the 1644 CE entry of Ambraseys (2009), this interpretation should be revised, and the 1656 CE earthquake is not to be associated with any local rupture in the Dead Sea.

https://doi.org/10.5194/nhess-2021-62
Preprint. Discussion started: 24 March 2021

Year CE or Century (marked C)	Class	Seismite correl. by site			Reference	Comments
		ZE[†]	EG[¥]	EF[°]		
33	B	+	+	+	MI,K&,W&,	Identified in all three seismites sites, varve-counted to 31 BCE
100~	B	-	2	-	MI,AM	Seismites ~90 and ~112; questionable archaeologic evidence
~175	B	-	+	-	MI	A seismite; no historic or archeological support
363	C	-	-	+	K&,A&	A seiche in the Dead Sea, a seismite at EF[°] (north Dead Sea)
419	C	+	+	+	KT/MI/K&	
551	A	+	+	+	PA,AM	
747/9,757	C	+	+	+	KT/MI/K&	
1033	C	?	+	+	KT/MI/K&	
~1150	A	+	-	/	AM,K&	I_0 IX - Mar Elias (& Qasr al-Yahud) monastries demolished
1293	C	+	+	+	K&	
1458	C	+	+	hiatus	MI	
1546	C	/	+		MI	
1712	A	/	+		MI	A& / I_0 VII - “ruined three Turkish houses in Jerusalem”
1834	C	+	+		KT,MI	
1903	R	m	m		A&,AM	I_0 VII Mt. of Olives; several shocks, I_0 up to VII over a large area
1927	C	+	+		KT,MI	AV / I_0 VII-VIII in and around Jerusalem (I_0 7.8 by GMPE)

Table A1: A list of earthquakes that could potentially damage Jerusalem. The classes denote the level of acceptance of damage to Jerusalem among the researchers: C - consensual; B - accepted by Belferman et al., 2018; A - amended here; R - rejected here.

Abbreviations and notes:

[†]ZE - Ze‘ elim Creek; [¥]EG - Ein Gedi core; °EF - Ein-Feshkhs Nature Reserve

https://doi.org/10.5194/nhess-2021-62
Preprint. Discussion started: 24 March 2021

Natural Hazards and Earth System Sciences Discussions

AM: Ambraseys, 2009; A&: Amiran et al., 1994; K&: Kagan et al., 2011; L&: Langgut et al. 2015; KT: Ken-Tor et al., 2004; MI: Migowski et al., 2004; PA: Parker, 1982; W&: Williams et al., 2012.

Year CE	Class	Seismite correl. by site			Reference	Comments
		ZE†	EG¥	EF°		
~659	R	-	+	+	L&,AM	Jordan Valley, possibly over 65 km NE of Jerusalem
808	S	/	-	?	A&	
1016	D	?	?	?	AM,A&	Damage to the Dome of Rock, no specific reference to shaking
1042	S	-	+	-	BM	Syria, off the Dead Sea transform
1060	S	/	-	+	A&,SB	The roof of Al-Aqsa collapsed
1063	R				A&,AM,SB	Syrian littoral
1068	D	+	+	+	AM	Neither of the two events can be associated with the Dead Sea
1105	D	?	?	?	A&,AM	“Strong” but “no damage recorded in the sources”
1114	D	+	+	?	A&,AM	1114 - no damage around the city, a swarm, Kingdom’s north
~1117	R	+		?	A&,AM	
1557	R				Am	Collapse in Jerusalem: a gun foundry, a forgery, an oven
1644	R	h	+*	h	Am	Some damage and death toll in Palestine, likely Seismite 6 of MI
1656	R	h	-	h	A&,AM,SB	Tripoli VII, Palestine IV, MI misidentified with Seismite 6
1817	R				AM	Two churches damaged in Jerusalem, Holy Sepulchre affected
1870	S	?	-	h	AM	Mediterranean source

Table A2: Events listed in some catalogs and subsequently skipped (Class S) or declined (Class D) by Ambraseys (2009), or rejected (Class R) in the present study.

https://doi.org/10.5194/nhess-2021-62
Preprint. Discussion started: 24 March 2021

Natural Hazards and Earth System Sciences
Discussions

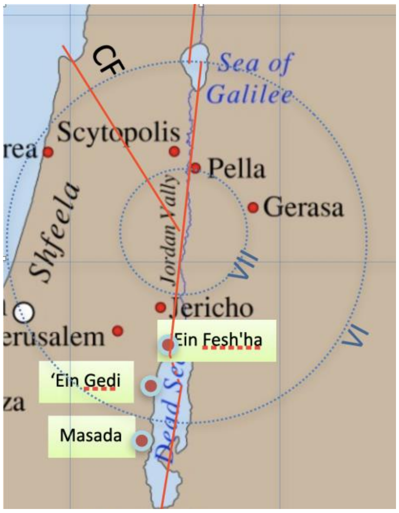

Figure A1: *A map showing the epicenter reconstructed by Langgut et al. (2015) for the 659/660 mainshock.*